MOLECULAR AND CELLULAR BIOLOGY, May 2009, p. 2390–2397 Vol. 29, No. 9
0270-7306/09/$08.00+0 doi:10.1128/MCB.01569-08

Altered States of Telomere Deprotection and the Two-Stage Mechanism of Replicative Aging[▽]

Ying Zou,[1]† Sandeep Misri,[2] Jerry W. Shay,[1] Tej K. Pandita,[2]‡ and Woodring E. Wright[1]‡*

Department of Cell Biology, University of Texas Southwestern Medical Center, Dallas, Texas,[1] and Radiation and Cancer Biology Division, Washington University School of Medicine, St. Louis, Missouri[2]

Received 7 October 2008/Returned for modification 28 December 2008/Accepted 5 February 2009

The molecular distinctions between mortality stages 1 (M1; senescence) and 2 (M2; crisis) of human replicative aging are ill defined. We demonstrate a qualitative difference between telomeric end associations at M1 and the end fusions that produce dicentric chromosomes and breakage-fusion cycles. Knockdown of ligase IV sufficient to completely inhibit radiation-induced dicentric chromosome formation had no effect on the frequency of telomere associations (TAs), establishing that TAs are not covalent conventional nonhomologous end-joining (NHEJ) products. TAs preceded and were more numerous than dicentric chromosomes. Cells initially tolerated dicentric chromosomes without dying, but eventually, a combination of too many TAs and dicentrics/complex chromosomal rearrangements resulted in apoptosis. We propose a working model in which end associations represent abortive DNA repair intermediates when the number of telomeric repeats is too small to completely inhibit DNA damage signaling but is sufficient to prevent the final covalent ligation step of NHEJ and induces the M1 checkpoint arrest in normal human cells. Rather than being all-or-none, telomere deprotection would thus proceed first through TAs before additional shortening leads to dicentric chromosomes. M2/crisis involves both qualitative changes (a shift from TAs to TAs plus dicentric chromosomes) and quantitative changes (an increase in the number of dysfunctional telomeres).

Normal diploid human fibroblasts have a limited capacity to divide in culture (19), which is thought to provide a barrier to the formation of cancer. Since each mutation probably requires 20 to 40 doublings to grow to a sufficient clonal population size for the next mutation to occur, a proliferative life span of less than 100 doublings would block precancerous cells with one or two mutations from progressing to frank malignancy (52). The broad outline of the molecular basis for replicative aging began to emerge when it was found that telomere length decreased with increasing cell doublings in vitro and with donor age in vivo (9, 17, 18, 24), suggesting that this shortening might count cell divisions. This concept was supported by showing that that the forced expression of the protein component of telomerase (hTERT) in human fibroblasts was sufficient to restore telomerase activity, maintain telomere length, and abolish the limits to cell proliferation (3, 45). The hypothesis that the primary role of telomerase expression in tumors was to permit escape from the replicative arrest imposed by telomere shortening (7, 23, 26) was confirmed by inhibiting telomerase in tumor cells and showing that this produced telomere shortening and eventual proliferative failure (15, 20, 54).

We formulated a two-stage model of replicative aging (49, 53) to explain the observation that viral proteins such as the simian virus 40 T antigen or human papillomavirus type 16 (HPV16) E6/E7 could extend the life span of human fibroblasts without immortalizing them. Our current interpretation of this model (50, 51) is that mortality stage 1 (M1) occurs when telomeres become sufficiently short to induce the cell cycle checkpoint activities that cause senescent growth arrest. Stasis (12), which can occur spontaneously due to inadequate culture conditions (31) or be induced at any population doubling (PD) level by overexpression of oncogenes (36, 55) or mitomycin C (32), is a type of senescence that is not due to short telomeres and does not represent M1. The checkpoint-blocking activities of T antigen or E6/E7 permit additional cell divisions beyond M1 until telomeres become so short that they can no longer protect the ends of the chromosomes. End-to-end fusions and chromosome breakage then result in apoptosis and mortality stage 2 (M2; crisis). Rare cells that express factors for maintaining telomeres, either by reactivating telomerase (major pathway) or a less-frequent recombination-based ALT (alternative lengthening of telomeres) pathway (4, 5), emerge from M2 in human fibroblasts with a frequency of approximately 10^{-7} (39, 40).

Dysfunctional telomeres can be found in DNA damage foci (8, 43), and specifically, the shortest telomeres are found in such foci as cells approach senescence (56), and they contribute to genomic instability following the introduction of oncogenes (10). Increased genomic instability has been shown to occur in mice developing short telomeres after several generations in the absence of telomerase, and this is associated with increased oncogenesis when combined with p53 mutations (6). This has led to the concept that replicative aging is a two-edged sword, in which the advantages of limiting the number of divisions as a tumor protection strategy is finely balanced against the genomic instability produced in checkpoint-abrogated cells when their telomeres get very short (1, 25).

A central unexplained facet of the two-stage model is the mechanism by which cells deal with their short telomeres be-

* Corresponding author. Mailing address: Department of Cell Biology, UT Southwestern Medical Center, 5323 Harry Hines Blvd., Dallas, TX 75390-9039. Phone: (214) 648-2933. Fax: (214) 648-8694. E-mail: woodring.wright@utsouthwestern.edu.

† Present address: Center for Human Genetics, Boston University School of Medicine, Boston, MA.

‡ These authors contributed equally to this work.

▽ Published ahead of print on 17 February 2009.

tween M1 and M2. If telomeres are sufficiently short to induce a DNA damage response at M1, why is the apoptosis response delayed for many doublings until M2? Is this simply a matter of a cell being able to tolerate a few unprotected ends but decompensating as more ends become dysfunctional with ongoing cell division? Are the short telomeres at M1 inducing breakage-fusion cycles that produce genomic instability during the extended life span? Alternatively, is there a difference in the degree of deprotection that occurs as telomeres shorten so that telomeres sufficiently short to generate a DNA damage signal (causing them to be found in damage foci produced at M1) are nonetheless protected from end fusion to other telomeres? In order to address these issues, we have monitored the cytogenetics of cells during the extended life span produced by the expression of HPV16 E6/E7. We observed increasing numbers of telomere associations (TAs; where the ends of chromosomes touch without a constriction at the junction, without any evidence of cytogenetic abnormalities) between M1 and M2. The accumulation of these associations did not affect the growth rate or increase apoptosis, although it was associated with an increase in anaphase bridges. Knockdown of the nonhomologous end-joining (NHEJ) enzyme ligase IV had no effect on the abundance of TAs, suggesting that TAs might represent DNA repair intermediates blocked from at least the final NHEJ step of covalent end-to-end fusions. The increase in dicentric chromosomes (end fusion) lagged approximately seven to eight doublings behind TAs. M2 occurred once cells with dicentric chromosomes divided enough times to form complex rearrangements and most cells contained both TAs and dicentric chromosomes. We suggest that telomeres can exist in two qualitatively different deprotected states, in which short telomeres enter a noncovalent structure (TA) that triggers a DNA damage response (M1) many doublings prior to a change in state that produces the onset of actual end fusion events (dicentric chromosomes) that eventually lead to cell death (M2). This model has important implications for understanding normal senescence and the ongoing presence of high levels of TAs in many cancer cells.

MATERIALS AND METHODS

Cell culture. BJ foreskin fibroblasts and derivatives of them were grown at 37°C in 5% CO_2 in a 4:1 mixture of Dulbecco's modified Eagle's medium and medium 199 containing 10% iron-supplemented calf serum (HyClone) and gentamicin (25 μg/ml; Sigma-Aldrich, St. Louis, MO). Cells were infected with a pLXSN retrovirus expressing HPV16 E6 and E7 proteins (16) approximately 30 doublings prior to senescence and selected on G418 (400 μg/ml) for 10 to 14 days. Metaphase spreads were then prepared as described below. The frequency of anaphase bridges was determined in dividing cultures fixed three times with methanol-acetic acid (3:1) in their original dish. The dish was then stained with 2% (vol/vol) Giemsa stain (Bio/medical Specialties, CA) in Gurr's buffer, pH 6.8. The frequency of apoptosis was determined by terminal deoxynucleotidyltransferase-mediated dUTP-biotin nick end-labeling analysis on cells growing on glass coverslips using a DNA fragmentation assay kit (Clontech Laboratories, Palo Alto, CA) according to the manufacturer's protocol.

Metaphase spread preparation and cytogenetics analysis. Cells plated at near confluence were incubated with colcemid (Invitrogen) the next day for 4 h. After trypsinization, cells were treated with hypotonic KCl buffer (0.075 M) for 30 min at 37°C and washed several times with methanol-acetic acid (3:1) until a clean, white cell pellet was obtained. Pellets were stored at −20°C. Cells were dropped onto slides and GTG banded using standard methods (14). Metaphase images were captured and analyzed using Microprobe software (Apply Imaging, Inc.) at the cytogenetics laboratory at the University of Texas Southwestern Medical Center.

Quantitative fluorescence in situ hybridization. After being washed with phosphate-buffered saline (PBS) for 15 min, 1-day-old slides were fixed in formaldehyde (4%) in PBS for 2 min, washed with PBS three times for 5 min, and treated with pepsin (Sigma) at 1 mg/ml at pH 2 for 10 min at 37°C. Formaldehyde fixation and washing steps were repeated and slides were dehydrated through an ethanol series (70%, 85%, and 100%) and air dried. The hybridization mixture (20 μl) contained 70% formamide, 15 ng 3′ Cy3-conjugated $(CCCTAA)_3$ 2′-deoxyoligonucleotide N3′→P′ phosphoramidate telomeric probe (kindly provided by Sergei Gryaznov, Geron Corp.), 0.25% (wt/vol) blocking reagent (Roche Molecular Biochemicals), and 5% $MgCl_2$ in 10 mM Tris, pH 7.2. This was added to the slide, denatured for 3 min at 78°C, annealed for 2 h at room temperature, and washed twice with 70% formamide, 0.1% bovine serum albumin, and 10 mM Tris, pH 7.2, and twice with 0.15 M NaCl, 0.05% Tween 20, and 0.05 M Tris. The slides were then dehydrated through an ethanol series (70%, 85%, and 100%) and air dried in the dark. Chromosomes were counterstained with Vectashield containing diamidino-phenylindole-dihydrochloride (DAPI) (0.6 μg/ml final concentration; Vector Laboratories) for chromosome identification. Slides were digitally imaged on a Zeiss Axioplan 2 microscope (63×, 1.4 numerical aperture, Plan-Apochromat oil immersion objective) with precision Cy3/DAPI band-pass filter sets. Cy3 and DAPI images were captured separately with a charge-coupled-device (Hamamatsu Photonics, Hamamatsu City, Japan) camera. Quantitative fluorescence in situ hybridization analysis was performed by ImageJ software (NIH). We used a clone of mouse NIH 3T3 cells as an internal control to compensate for day-to-day variation due to aging of the lamp and alignment of the optics, etc., and for conversion of the intensity measurements of human telomeres to kilobases (57). Chromosomes were identified through the banding patterns of the inverted DAPI image and karyotyped as described above.

Immunofluorescence. Cells grown on coverslips were rinsed with PBS, fixed in 4% paraformaldehyde in PBS at room temperature (RT) for 15 min, and then permeabilized in 0.1% Triton X-100 buffer in PBS at RT for 10 min. For dual immunostaining, cells were first blocked with 10% bovine serum albumin (Sigma) in PBS and then incubated at 37°C for 1 h with a mixture of primary antibodies. Anti-phospho-histone H2AX antibody (Upstate Biologicals Inc., Lake Placid, NY) was used at a dilution of 1:50, and anti-Mre11 antibody (12D7; GeneTex, Inc., San Antonio, TX) was used at a dilution of 1:200. The mouse anti-53BP1 antibody was a gift from J. Chen (Mayo Clinic and Foundation, Rochester, MN). Following incubation, cells were washed with PBS and incubated with fluorescein isothiocyanate-conjugated donkey anti-rabbit and/or fluorescein isothiocyanate-conjugated donkey anti-goat and/or tetramethyl rhodamine isothiocyanate-conjugated donkey anti-mouse antibodies (1:200 dilution; Jackson Laboratories, Bar Harbor, ME) at RT for 1 h. After being washed, the cells were counterstained with Vectashield containing DAPI (Vector Laboratories) for 2 min at RT, washed with PBS, mounted on glass slides, and imaged using a Zeiss Axioplan 2 microscope.

G_1 chromosome end association analysis. Factors from mitotic cells cause interphase chromatin to undergo a prophase-like reaction and form prematurely condensed chromosomes (22). Premature chromosome condensation (PCC) was performed by fusing mitotic CHO cells to interphase BJ fibroblasts and combined with in situ hybridization to a whole human genome probe as described previously (29, 37). Slides were coded and scored by researchers without knowledge of the source.

Knockdown of ligase IV. BJ B14 cells (28) were infected with the pLXSN retrovirus expressing HPV16 E6 and E7 proteins (16) and selected for G418 resistance. Both populations were then infected with a retrovirus expressing an NHEJ reporter that contained an I-SceI restriction site, similar to the DR-green fluorescent protein reporters previously described (30). Because it proved much more convenient to monitor NHEJ by the response to irradiation rather than by following the transfection with I-SceI, this reporter system was not used but nonetheless provided duplicate populations for comparison. Aliquots of three populations were then infected with a retrovirus with the dominant negative hTERT D869A mutation in the reverse transcriptase motif C domain (2, 48).

Ligase IV small interfering RNA (siRNA) and control Luc siRNA were obtained from Dharmacon RNAi Technologies (Lafayette, CO) and used at a final concentration of 1.4 μM. Ligase IV levels were determined 48 h after transfection by Western analysis using ligase IV antibody (Santa Cruz Biotechnology, Inc., Santa Cruz, CA). Cells were irradiated with 2 Gy of X rays at the dose rate of 1 Gy/min and incubated for 12 h, and then colcemid was added and metaphase spreads were made as described previously (38). After standard Giemsa staining, metaphase spreads were analyzed for chromosome end associations, which include association between chromatids of different chromosomes as well as sister chromatids and were different from dicentrics as shown in Fig. 1A. Samples were coded and scored by researchers without knowledge of prior treatments to prevent experimental bias.

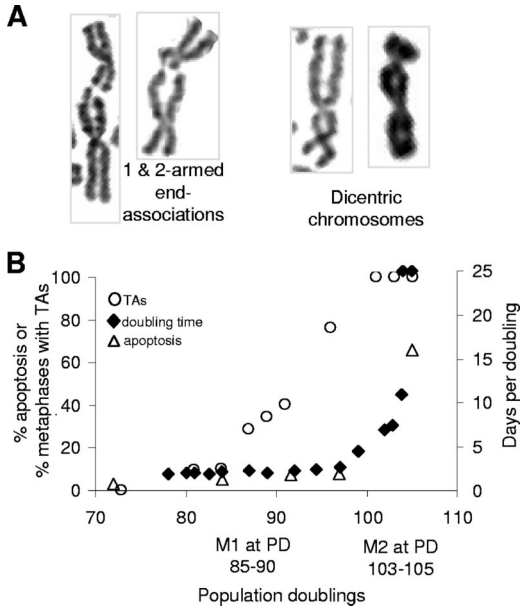

FIG. 1. TAs between M1 and M2. (A) Examples of TAs (showing constrictions at the junctions) and dicentrics (showing uniform chromatid diameters between the two centromeres). (B) The frequency of end associations, the PD times, and apoptosis percentages are compared as a function of PDs in BJ fibroblasts expressing E6/E7. The approximate PD at which M1 would have occurred in cells lacking E6/E7 is shown. The growth rate is the inverse of the number of days per PD.

RESULTS

TAs during the progression between M1 and M2. End associations between chromosomes were scored as TAs if either one or both chromatids from two chromosomes were involved, a clear constriction indicating the junction of the two chromatids was seen, and no additional chromosome anomalies were observed. They were scored as dicentric chromosomes if both chromatid arms from two chromosomes were involved and the chromatids exhibited a relatively uniform diameter between the two centromeres (Fig. 1A). Additional chromosome structural anomalies, such as deletions and/or duplications of genomic segments, were frequently observed in dicentric chromosomes. Figure 1B compares the frequencies of TAs with the PD times and the percentages of apoptotic cells during the period of extended life span. TAs increased during the extended life span without affecting viability or growth rate, such that at PD 96, almost 80% of the cells had TAs without any changes in doubling time.

TAs are not dependent on ligase IV. The presence of frequent telomere end associations occurred without an increase in apoptosis, the PD time, or an immediate appearance of dicentric chromosomes or other chromosomal abnormalities, such as translocations or deletions (Fig. 2). These observations suggested that end associations might represent intermediates in an abortive repair process rather than covalently joined chromosomes. This could occur if a telomere still had sufficient telomeric sequences to bind factors that partially inhibited the DNA repair response even after it had shortened enough to generate damage signals. Uncapped telomeres generate DNA damage signals that are repaired by NHEJ (11, 41). In order to examine if the TAs observed between M1 and M2 represented noncovalent complexes, we examined the consequences of knockdown of ligase IV, the ligase required for the final step in NHEJ. The telomere length constantly changes between M1 and M2, and it would be technically challenging to use cells in which the number of TAs changed with every few divisions. We thus examined TAs in a strain of BJ fibroblasts with very short telomeres. BJ B14 cells express extremely low levels of telomerase so that only the shortest telomeres can be maintained. As a consequence, the longer telomeres shortened until they could effectively recruit telomerase, resulting in a normal cell with an average telomere length of only ~3.5 kb, rather than the 6 to 7 kb normally seen at senescence (28).

We introduced HPV16 E6/E7 and/or a dominant negative telomerase with a mutation in one of the reverse transcriptase domains (2, 48) in case these factors were needed to produce an adequate number of TAs. In addition, we infected some cells with what turned out to be an irrelevant reporter system (see Materials and Methods), which provided duplicate samples and controls. All of these cells were transduced with a ligase IV siRNA. Twenty-four hours later, aliquots of each group were irradiated with 200 rads in order to induce chromosome breaks and the formation of dicentric chromosomes, and 1 day later, the frequencies of dicentric chromosomes and TAs were examined. Figure 3A demonstrates a >70% decrease in the amount of ligase IV protein. Figure 3B shows that this decrease was sufficient to block NHEJ, since the frequency of dicentric chromosomes was reduced to the background level present in the absence of irradiation. In contrast to the behavior of dicentric chromosomes, the frequency of TAs remained completely unaffected by the ligase knockdown, showing no significant decrease in any of the seven different populations examined (Fig. 3C). Cells were examined within approximately six doublings of introducing the dominant-negative hTERT, and as expected, the additional shortening occurring during these doublings caused an increase in TAs. The increased TAs in these cells also remained unaffected by the knockdown of ligase IV. We conclude that ligase IV and thus covalent end fusion by conventional NHEJ are not required for the formation of TAs. This experiment does not address whether or not TAs represent the consequences of a blocked NHEJ complex or other types of repair intermediates, such as homologous recombination.

G_1 TAs correlate with DNA damage foci. Telomeres short enough to produce end associations that separated during mitosis should still generate DNA damage signals and create new end associations in G_1. We thus examined the presence of end associations in G_1 and the appearance of DNA damage foci.

G_1 TAs were observed by fusing interphase BJ E6/E7-expressing cells to mitotic CHO cells, thus producing prematurely condensed chromosomes (22, 37). The number of end associations observed in G_1 by PCC is shown in Fig. 4 and compared to mitotic TAs Fig. 5A. Although G_1 TAs were minimal prior to M1, they increased much more rapidly than mitotic TAs. The structure of G_1 TAs is unknown, and it is possible they do not represent the same phenomenon as metaphase TAs. However, if they are related, the increased numbers of G_1 end associations in comparison to mitotic end associations implies that the sensitivity of detection by PCC is

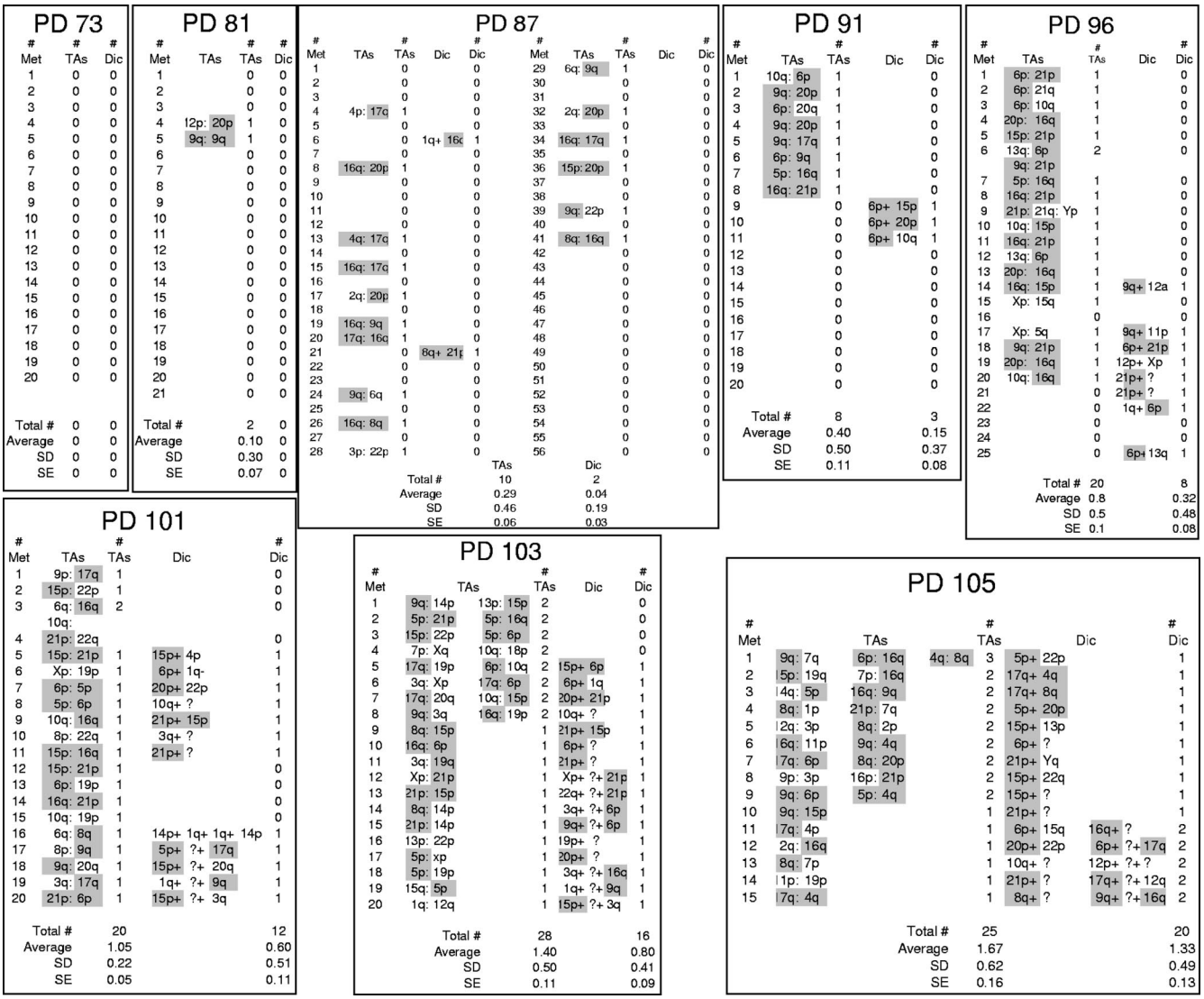

PD 73

# Met	# TAs	# Dic
1	0	0
2	0	0
3	0	0
4	0	0
5	0	0
6	0	0
7	0	0
8	0	0
9	0	0
10	0	0
11	0	0
12	0	0
13	0	0
14	0	0
15	0	0
16	0	0
17	0	0
18	0	0
19	0	0
20	0	0
Total #	0	0
Average	0	0
SD	0	0
SE	0	0

PD 81

# Met	TAs	# TAs	# Dic
1		0	0
2		0	0
3		0	0
4	12p: 20p	1	0
5	9q: 9q	1	0
6		0	0
7		0	0
8		0	0
9		0	0
10		0	0
11		0	0
12		0	0
13		0	0
14		0	0
15		0	0
16		0	0
17		0	0
18		0	0
19		0	0
20		0	0
21		0	0
Total #		2	0
Average		0.10	0
SD		0.30	0
SE		0.07	0

PD 87

# Met	TAs	# TAs	Dic	# Dic	# Met	TAs	# TAs	Dic	# Dic
1		0		0	29	6q: 9q	1		0
2		0		0	30		0		0
3		0		0	31		0		0
4	4p: 17q	1		0	32	2q: 20p	1		0
5		0		0	33		0		0
6		0	1q+ 16q	1	34	16q: 17q	1		0
7		0		0	35		0		0
8	16q: 20p	1		0	36	15p: 20p	1		0
9		0		0	37		0		0
10		0		0	38		0		0
11		0		0	39	9q: 22p	1		0
12		0		0	40		0		0
13	4q: 17q	1		0	41	8q: 16q	1		0
14		0		0	42		0		0
15	16q: 17q	1		0	43		0		0
16		0		0	44		0		0
17	2q: 20p	1		0	45		0		0
18		0		0	46		0		0
19	16q: 9q	1		0	47		0		0
20	17q: 16q	1		0	48		0		0
21		0	8q+ 21p	1	49		0		0
22		0		0	50		0		0
23		0		0	51		0		0
24	9q: 6q	1		0	52		0		0
25		0		0	53		0		0
26	16q: 8q	1		0	54		0		0
27		0		0	55		0		0
28	3p: 22p	1		0	56		0		0
		TAs		Dic					
Total #		10		2					
Average		0.29		0.04					
SD		0.46		0.19					
SE		0.06		0.03					

PD 91

# Met	TAs	# TAs	Dic	# Dic
1	10q: 6p	1		0
2	9q: 20p	1		0
3	6p: 20q	1		0
4	9q: 20p	1		0
5	9q: 17q	1		0
6	6p: 9q	1		0
7	5p: 16q	1		0
8	16q: 21p	1		0
9		0	6p+ 15p	1
10		0	6p+ 20p	1
11		0	6p+ 10q	1
12		0		0
13		0		0
14		0		0
15		0		0
16		0		0
17		0		0
18		0		0
19		0		0
20		0		0
Total #		8		3
Average		0.40		0.15
SD		0.50		0.37
SE		0.11		0.08

PD 96

# Met	TAs	# TAs	Dic	# Dic
1	6p: 21p	1		0
2	6p: 21q	1		0
3	6p: 10q	1		0
4	20p: 16q	1		0
5	15p: 21p	1		0
6	13q: 6p	2		0
	9q: 21p			
7	5p: 16q	1		0
8	16q: 21p	1		0
9	21p: 21q: Yp	1		0
10	10q: 15p	1		0
11	16q: 21p	1		0
12	13q: 6p	1		0
13	20p: 16q	1		0
14	16q: 15p	1	9q+ 12a	1
15	Xp: 15q	1		0
16		0		0
17	Xp: 5q	1	9q+ 11p	1
18	9q: 21p	1	6p+ 21p	1
19	20p: 16q	1	12p+ Xp	1
20	10q: 16q	1	21p+ ?	1
21		0	21p+ ?	1
22		0	1q+ 6p	1
23		0		0
24		0		0
25		0	6p+ 13q	1
Total #		20		8
Average		0.8		0.32
SD		0.5		0.48
SE		0.1		0.08

PD 101

# Met	TAs	# TAs	Dic	# Dic
1	9p: 17q	1		0
2	15p: 22p	1		0
3	6q: 16q	2		0
	10q:			
4	21p: 22q			0
5	15p: 21p	1	15p+ 4p	1
6	Xp: 19p	1	6p+ 1q-	1
7	6p: 5p	1	20p+ 22p	1
8	5p: 6p	1	10q+ ?	1
9	10q: 16q	1	21p+ 15p	1
10	8p: 22q	1	3q+ ?	1
11	15p: 16q	1	21p+ ?	1
12	15p: 21p	1		0
13	6p: 19p	1		0
14	16q: 21p	1		0
15	10q: 19p	1		0
16	6q: 8q	1	14p+ 1q+ 1q+ 14p	1
17	8p: 9q	1	5p+ ?+ 17q	1
18	9q: 20q	1	15p+ ?+ 20q	1
19	3q: 17q	1	1q+ ?+ 9q	1
20	21p: 6p	1	15p+ ?+ 3q	1
Total #		20		12
Average		1.05		0.60
SD		0.22		0.51
SE		0.05		0.11

PD 103

# Met	TAs	TAs	# TAs	Dic	# Dic
1	9q: 14p	13p: 15p	2		0
2	5p: 21p	5p: 16q	2		0
3	15p: 22p	5p: 6p	2		0
4	7p: Xq	10q: 18p	2		0
5	17q: 19p	6p: 10q	2	15p+ 6p	1
6	3q: Xp	17q: 6p	2	6p+ 1q	1
7	17q: 20q	10q: 15p	2	20p+ 21p	1
8	9q: 3q	16q: 19p	2	10q+ ?	1
9	8q: 15p		1	21p+ 15p	1
10	16q: 6p		1	6p+ ?	1
11	3q: 19q		1	21p+ ?	1
12	Xp: 21p		1	Xp+ ?+ 21p	1
13	21p: 15p		1	22q+ ?+ 21p	1
14	8q: 14p		1	3q+ ?+ 6p	1
15	21p: 14p		1	9q+ ?+ 6p	1
16	13p: 22p		1	19p+ ?	1
17	5p: xp		1	20p+ ?	1
18	5p: 19p		1	3q+ ?+ 16q	1
19	15q: 5p		1	1q+ ?+ 9q	1
20	1q: 12q		1	15p+ ?+ 3q	1
Total #			28		16
Average			1.40		0.80
SD			0.50		0.41
SE			0.11		0.09

PD 105

# Met	TAs	TAs	# TAs	Dic	# Dic
1	9q: 7q	6p: 16q	3	5p+ 22p	1
2	5p: 19q	7p: 16q	2	17q+ 4q	1
3	4q: 5p	16q: 9q	2	17q+ 8q	1
4	8q: 1p	21p: 7q	2	5p+ 20p	1
5	2q: 3p	8q: 2p	2	15p+ 13p	1
6	6q: 11p	9q: 4q	2	6p+ ?	1
7	7q: 6p	8q: 20p	2	21p+ Yq	1
8	9p: 3p	16p: 21p	2	15p+ 22q	1
9	9q: 6p	5p: 4q	2	15p+ ?	1
10	9q: 15p		1	21p+ ?	1
11	7q: 4p		1	6p+ 15q	16q+ ? 2
12	2q: 16q		1	20p+ 22p	6p+ ?+ 17q 2
13	8q: 7p		1	10q+ ?	12p+ ?+ ? 2
14	1p: 19p		1	21p+ ?	17q+ ?+ 12q 2
15	7q: 4q		1	8q+ ?	9q+ ?+ 16q 2
Total #			25		20
Average			1.67		1.33
SD			0.62		0.49
SE			0.16		0.13

FIG. 2. Data for TAs and dicentric chromosomes (Dic). TAs and dicentrics were scored between PD 73 and 103. Data for specific chromatids involved in each event are shown. The 10 shortest BJ telomeres (21p, 6p, 17q, 16q, 9q, 15p, 20p, 8q, 4q, and 5p) (56) are highlighted in gray. Approximately 90% of all events involve at least one of these ends. Met, metaphase; SD, standard deviation; SE, standard error.

greater than in metaphase spreads, that many of the G_1 associations are disrupted during replication and do not reform, or that they are sufficiently weak that many of them are disrupted during G_2 or metaphase spread preparation (29).

The presence of DNA damage foci was analyzed by staining cells with antibodies to a variety of factors implicated in the repair response (Fig. 5B). γ-H2AX-positive DNA damage foci increase when cells reach replicative senescence (8). Normal diploid BJ fibroblasts (without HPV E6/E7) showed less than 0.1 focus per cell 20 doublings prior to senescence. This increases to one or two foci per cell at senescence (56). At low levels of DNA damage, the number of repair foci corresponds to the calculated number of induced lesions (33). Figure 5C shows the number of DNA damage foci per cell as a function of PD and demonstrates that the number of DNA damage foci corresponded closely to the number of TAs observed in G_1. The number occurring at the predicted M1 (PD 85 to 90; one to two foci per cell) corresponded to what was observed in normal BJ fibroblasts at M1 without E6/E7 (56). The appearance of damage foci and specific end associations at M1 was associated with the frequency of signal-free ends on a group of 10 chromosomes with the shortest telomeres (43, 56) and thus very limited amounts of remaining TTAGGG repeats. Although we were able detect weak telomeric repeat signals at the junctions of 50% of the TAs by in situ hybridization, we were unable to use immunocytochemistry to demonstrate significant colocalization of TRF1 antibody staining with these DNA damage foci (data not shown). Although we cannot directly demonstrate that G_1 TAs are located in these DNA damage foci, their absence prior to M1 and the quantitative equivalence in the increases of both as a function of doublings support this interpretation.

Dicentric chromosomes and M2. The frequency of dicentric chromosomes between M1 and M2 is shown in Fig. 6. At PD

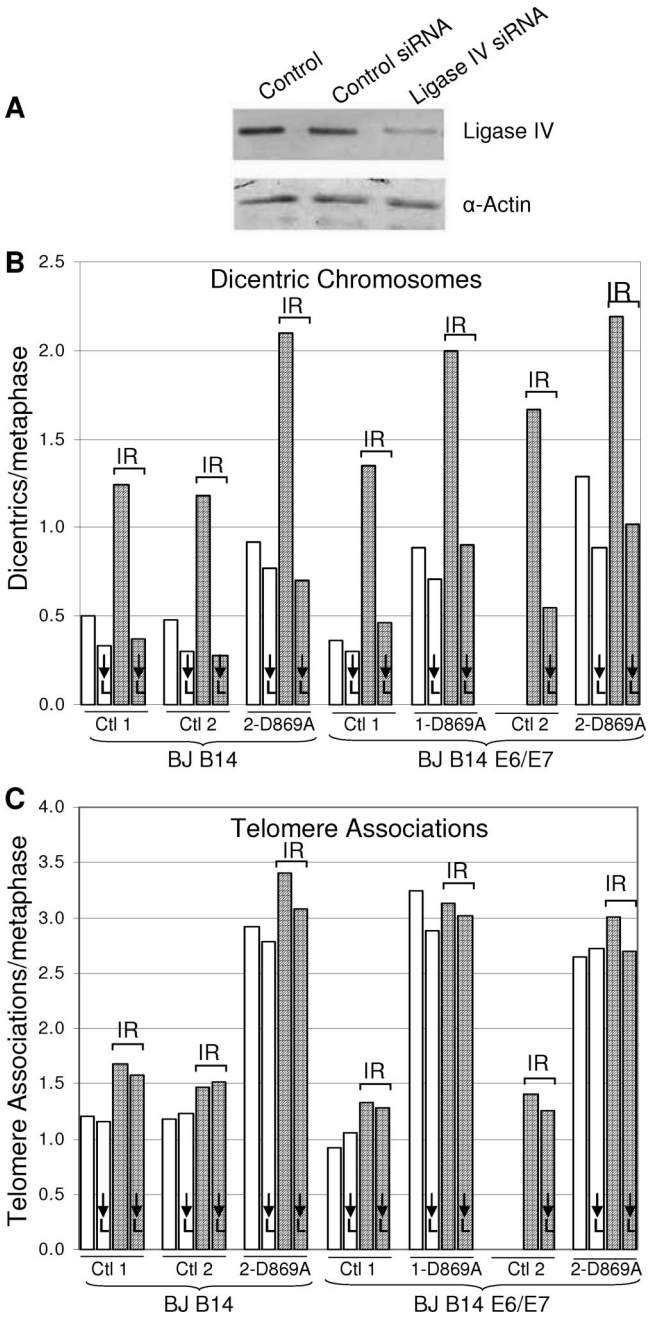

FIG. 3. TAs are not dependent on ligase IV. (A) Cells transfected with an siRNA against ligase IV show a >70% decrease in protein expression 48 h after transfection by Western blotting compared to cells transfected with a control siRNA. α, anti. (B and C) Cells transfected with control or ligase IV siRNAs were exposed to 200 rads of gamma irradiation (IR) 24 h after transfection. Metaphase spreads were collected 24 later and analyzed for dicentric chromosomes (B) or TAs (C). The numbers 1 and 2 (e.g., for controls 1 [Ctl 1] and 2 [Ctl 2]) represent cells infected with and without a reporter vector, respectively, that was not used in the analysis and which thus serve as duplicate populations. Ligase IV knockdown cells are indicated by ↓L. Two samples of nonirradiated BJ B14 E6/E7-expressing control 2 cells were lost and thus not analyzed. A level of knockdown sufficient to completely block dicentric chromosome formation had no effect on TAs.

PD 39
Cells scored =202
Cells without TAs =198
Cells with TAs = 4
Maximum TAs per cell = 1
TAs per cell = 0.02

# TAs /cell	# of cells	Tot TAs
0	198	0
1	4	4
Tot	202	4
Av.		0.02
SD		0.14
SE		0.01

PD 61
Cells scored= 220
Cells without TAs =213
Cells with TAs = 7
Maximum TAsper cell = 1
TAs per cell = 0.03

# TAs /cell	# of cells	Tot TAs
0	213	0
1	7	7
Tot	220	7
Av.		0.03
SD		0.18
SE		0.01

PD 85
Cells scored =102
Cells without TAs =75
Cells with TAs = 27
Maximum TAs per cell = 3
TAs per cell = 0.4

# TAs /cell	# of cells	Tot TAs
0	75	0
1	16	16
2	9	18
3	2	6
Tot	102	40
Av.		0.4
SD		0.7
SE		0.1

PD 90
Cells scored = 60
Cells without TAs =29
Cells with TAs = 31
Maximum TAs per cell = 6
TAs per cell = 1.25

# TAs /cell	# of cells	Tot TAs
0	29	0
1	8	8
2	11	22
3	7	21
4	2	8
5	2	10
6	1	6
Tot	60	75
Av.		1.25
SD		1.536
SE		0.198

PD 98
Cells scored =62
Cells without TAs =21
Cells with TAs = 41
Maximum TAs per cell = 9
TAs per cell = 3.42

# TAs /cell	# of cells	Tot TAs
0	21	0
1	5	5
2	3	6
3	4	12
4	3	12
5	4	20
6	7	42
7	8	56
8	4	32
9	3	27
Tot	62	212
Av.		3.4
SD		3.2
SE		0.4

PD 105
Cells scored= 49
Cells without TAs = 13
Cells with TAs = 36
Maximum TAs per cell = 11
TAsper cell = 5.12

# TAs /cell	# of cells	Tot TAs
0	13	0
1	2	2
2	1	2
3	2	6
4	1	4
5	2	10
6	4	24
7	8	56
8	5	40
9	5	45
10	4	40
11	2	22
Tot	49	251
Av.		5.12
SD		3.84
SE		0.55

FIG. 4. End associations during G_1. Telomeric end associations in G_1 were determined by inducing PCC by fusing interphase BJ E6/E7-expressing cells to mitotic CHO cells. The frequencies of telomeric end associations in G_1 are shown at different PDs. Tot, total; Av., average; SD, standard deviation; SE, standard error.

96, 30% of the cells at metaphase contained dicentric chromosomes without any change in the growth rate. This suggests that cells can survive for at least several divisions in the presence of one dicentric chromosome/cell (we never observed more than one per cell until PD 105 [Fig. 2]) in the absence of p53 and cell cycle checkpoints due to the presence of HPV16 E6/E7. Complex chromosome arrangements as a result of breakage-fusion cycles first appeared at PD 101 (Fig. 2 and 6A), and their increase paralleled the increase in PD times. These complex rearrangements thus serve as a marker for the onset of M2.

Anaphase bridges have frequently been used as a surrogate for end fusions and chromosome instability (27, 35). The numbers of anaphase bridges were very high in these cells even at PD 73, well before any TAs or dicentrics were present, presumably due to the inhibition of checkpoint functions by HPV16 E6/E7 proteins and DNA damage at nontelomeric sites. The frequency of anaphase bridges rose to almost 70% by PD 87 (Fig. 6C), when TAs were present in 34% of the cells at metaphase while dicen-

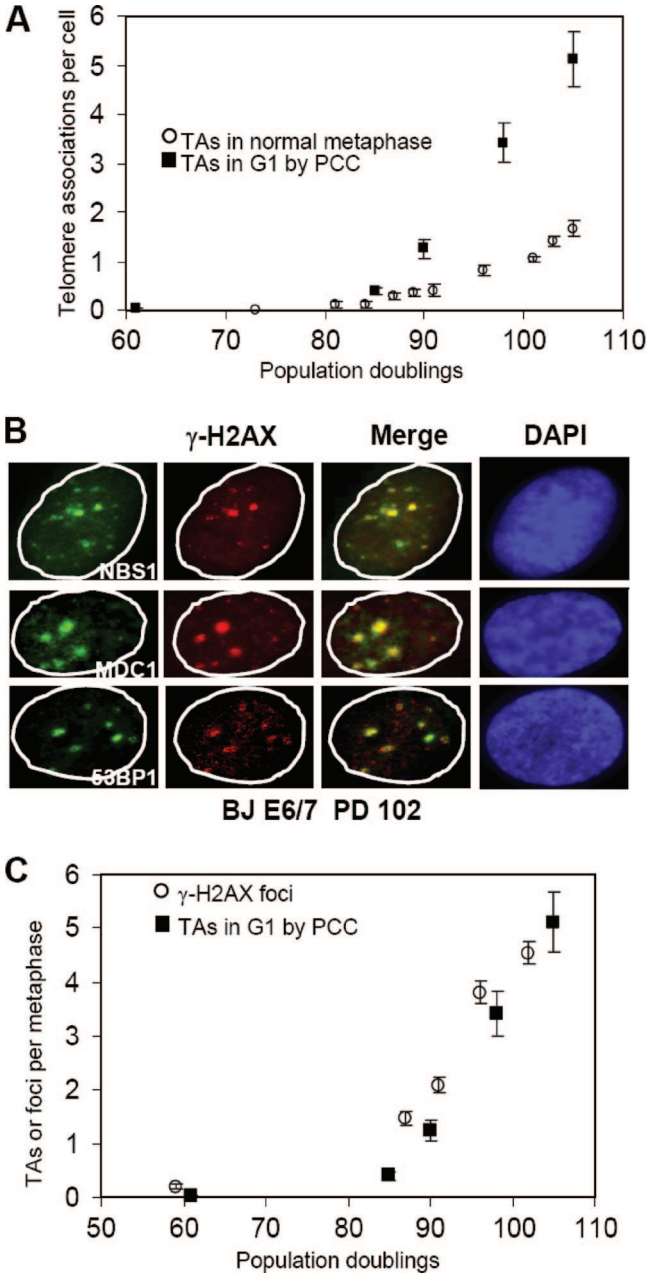

FIG. 5. End associations and DNA damage foci. (A) G_1 TAs appear at the same time but are three to four times more numerous than metaphase TAs. Note the change in scale from Fig. 1B. Means ± standard errors are shown. (B) Examples of DNA damage foci coexpressing γ-H2AX, NBS1, MDC1, or 53BP1. (C) The increases in DNA damage foci monitored by γ-H2AX staining (average of 200 nuclei) are quantitatively equivalent to the increases in G_1 TAs. Means ± standard errors are shown.

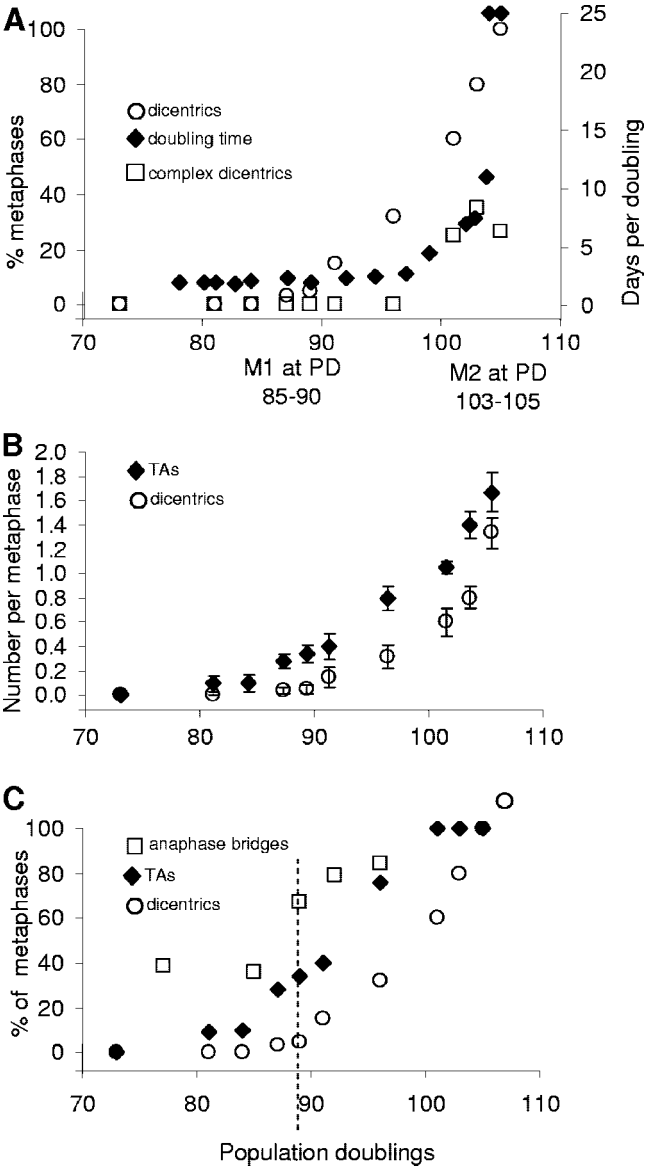

FIG. 6. Comparison of dicentric chromosomes and TAs. (A) The frequency of cells at metaphase containing simple dicentric chromosomes or those with complex rearrangements is compared to the PD time. The appearance of complex dicentrics occurs at the same time as M2/crisis. (B) The frequencies of TAs and dicentrics are compared. TAs precede and are more numerous than dicentrics. Data are from Fig. 2. Means ± standard errors are shown. (C) The presence of anaphase bridges is compared to that of TAs and dicentric chromosomes. A high baseline level of TAs is present at PD 77 prior to the appearance of TAs or dicentrics. The dashed vertical line indicates the PD at which anaphase bridges and TAs have increased without an increase in dicentric chromosomes.

trics were still close to baseline. This suggests that TAs may contribute to anaphase bridge formation.

DISCUSSION

The present results demonstrate that telomeres can exist in at least three states with respect to end protection: (i) long enough to be fully masked, (ii) short enough to produce damage signals and noncovalent TAs, and (iii) so short that they lose their end-protective function and cause end fusions. Rather than being simply a quantitative change (one or a few unprotected ends at M1 versus many at M2), the pattern of accumulation of TAs and dicentrics suggests that both qualitative and quantitative changes are occurring. Using subtelomeric probes, we have previously shown that the shortest telo-

meres appear in DNA damage foci as cells approach senescence, and senescent cells contained one or two foci/cell (56). In the present study, 40% of the cells in metaphase contained TAs (Fig. 1B) when BJ E6/E7-expressing cells contained averages of one to two DNA damage foci/cell (PD 85 to 90, when M1 occurred in control uninfected cells; Fig. 5C), suggesting that M1 occurred when telomeres became sufficiently short to induce both damage foci and TAs. As cells progressed between M1 and M2, both TAs and dicentrics increased, with the increase in TAs always preceding the increase in dicentric chromosomes. The cells tolerated these aberrations remarkably well, with no increase in growth rate or apoptosis until approximately PD 100, when 100% of the cells contained TAs and 60% contained dicentrics. Beyond PD 100, the growth rate decreased dramatically (the PD time increased) and the number of chromosomes exhibiting complex rearrangements increased in parallel. This suggests that M2 is caused by a combination of the changes occurring after several breakage-fusion cycles of dicentric chromosomes and having too many end abnormalities.

The current literature on telomeres has largely discussed end protection as an all-or-none state in which telomeres are either properly packaged or in a form that causes them to become fused by NHEJ to other chromosomes. The present results demonstrate that human telomere uncapping proceeds through at least two states, the first of which does not lead to cytologically detectable breakage-fusion cycles for many divisions. This is consistent with many other observations of the behavior of TAs in tumor cells. Knockdown of Pot1 (21) produces an increase in TAs and telomere-induced DNA damage foci in the absence of actual end fusions, similar to what we have observed here. Overexpression of a TRF2 that lacks the basic domain (44) also produces telomere dysfunction without end fusions. The knockdown of Pot1 leads to short overhangs, while the basic domain of TRF2 has been implicated in the formation of t-loops (13, 42, 47). Whether either of these manipulations models some of the events occurring between M1 and M2 remains to be seen. If NHEJ is involved in the formation of TAs, their ability to form in the absence of covalent linkage by ligase IV suggests a new regulatory influence of telomeres on the process of NHEJ.

Anaphase bridges have been used as a surrogate marker for end fusion events to support the contention that short telomeres are contributing to the ongoing genomic instability present in tumor cells (35, 46). Anaphase bridges did increase with the onset of end associations (Fig. 6C), suggesting that the structures holding telomeres together in TAs resolved only late and caused a delay in the separation of the two chromosomes. However, anaphase bridges were also high even at PD 77, many PDs before TAs increased at PD 87. This implies that nontelomeric chromosome damage can also lead to anaphase bridges in cells that lack normal DNA damage checkpoint controls. Furthermore, anaphase bridges increased between M1 and M2 without any significant increase in genomic instability. Anaphase bridges thus should be considered an only moderately reliable indicator of potential telomere-driven genomic instability in tumor cells.

Our previous understanding of the two-stage model of replicative aging, the events inducing M1, and the differences between M1 and M2 were quite vague, leading some authors to even claim that M1 and M2 were essentially the same phenomenon (34). The present results demonstrate there are both qualitative and quantitative differences between M1 and M2. The observation that end associations separate without overt breakage-fusion events and their formation is not dependent on ligase IV establishes the presence of a partially capped state distinct from fully unprotected ends, and its molecular definition will be important for models of telomere structure and function and the changes that initiate a DNA damage signal in comparison to those that result in end fusion. It is hoped that our increasing understanding of the molecular details of these processes will contribute to our ability to manipulate telomere biology for therapeutic purposes.

ACKNOWLEDGMENTS

This work was supported by NIH grants AG07992 (to W.E.W. and J.W.S.) and CA10445 and CA123232 (to T.K.P.).

We thank G. Sharma for technical help.

REFERENCES

1. **Artandi, S. E., and R. A. DePinho.** 2000. A critical role for telomeres in suppressing and facilitating carcinogenesis. Curr. Opin. Genet. Dev. **10:** 39–46.
2. **Bechter, O. E., Y. Zou, W. Walker, W. E. Wright, and J. W. Shay.** 2004. Telomeric recombination in mismatch repair deficient human colon cancer cells after telomerase inhibition. Cancer Res. **64:**3444–3451.
3. **Bodnar, A. G., M. Ouellette, M. Frolkis, S. E. Holt, C. P. Chiu, G. B. Morin, C. B. Harley, J. W. Shay, S. Lichtsteiner, and W. E. Wright.** 1998. Extension of life-span by introduction of telomerase into normal human cells. Science **279:**349–352.
4. **Bryan, T. M., A. Englezou, L. Dalla-Pozza, M. A. Dunham, and R. R. Reddel.** 1997. Evidence for an alternative mechanism for maintaining telomere length in human tumors and tumor-derived cell lines. Nat. Med. **3:**1271–1274.
5. **Bryan, T. M., A. Englezou, J. Gupta, S. Bacchetti, and R. R. Reddel.** 1995. Telomere elongation in immortal human cells without detectable telomerase activity. EMBO J. **14:**4240–4248.
6. **Chin, L., S. E. Artandi, Q. Shen, A. Tam, S. L. Lee, G. J. Gottlieb, C. W. Greider, and R. A. DePinho.** 1999. p53 deficiency rescues the adverse effects of telomere loss and cooperates with telomere dysfunction to accelerate carcinogenesis. Cell **97:**527–538.
7. **Counter, C. M., H. W. Hirte, S. Bacchetti, and C. B. Harley.** 1994. Telomerase activity in human ovarian carcinoma. Proc. Natl. Acad. Sci. USA **91:** 2900–2904.
8. **d'Adda di Fagagna, F., P. M. Reaper, L. Clay-Farrace, H. Fiegler, P. Carr, T. Von Zglinicki, G. Saretzki, N. P. Carter, and S. P. Jackson.** 2003. A DNA damage checkpoint response in telomere-initiated senescence. Nature **426:** 194–198.
9. **de Lange, T., L. Shiue, R. M. Myers, D. R. Cox, S. L. Naylor, A. M. Killery, and H. E. Varmus.** 1990. Structure and variability of human chromosome ends. Mol. Cell. Biol. **10:**518–526.
10. **der-Sarkissian, H., S. Bacchetti, L. Cazes, and J. A. Londono-Vallejo.** 2004. The shortest telomeres drive karyotype evolution in transformed cells. Oncogene **23:**1221–1228.
11. **Dimitrova, N., and T. de Lange.** 2006. MDC1 accelerates nonhomologous end-joining of dysfunctional telomeres. Genes Dev. **20:**3238–3243.
12. **Drayton, S., and G. Peters.** 2002. Immortalisation and transformation revisited. Curr. Opin. Genet. Dev. **12:**98–104.
13. **Fouché, N., A. J. Cesare, S. Willcox, S. Ozgur, S. A. Compton, and J. D. Griffith.** 2006. The basic domain of TRF2 directs binding to DNA junctions irrespective of the presence of TTAGGG repeats. J. Biol. Chem. **281:**37486–37495.
14. **Gustashaw, K. M.** 1997. Chromosome stains. Lippincott-Raven, Philadelphia, PA.
15. **Hahn, W. C., S. A. Stewart, M. W. Brooks, S. G. York, E. Eaton, A. Kurachi, R. L. Beijersbergen, J. H. Knoll, M. Meyerson, and R. A. Weinberg.** 1999. Inhibition of telomerase limits the growth of human cancer cells. Nat. Med. **5:**1164–1170.
16. **Halbert, C. L., G. W. Demers, and D. A. Galloway.** 1992. The E6 and E7 genes of human papillomavirus type 6 have weak immortalizing activity in human epithelial cells. J. Virol. **66:**2125–2134.
17. **Harley, C. B., A. B. Futcher, and C. W. Greider.** 1990. Telomeres shorten during ageing of human fibroblasts. Nature **345:**458–460.
18. **Hastie, N. D., M. Dempster, M. G. Dunlop, A. M. Thompson, D. K. Green, and R. C. Allshire.** 1990. Telomere reduction in human colorectal carcinoma and with ageing. Nature **346:**866–868.

19. **Hayflick, L., and P. S. Moorhead.** 1961. The serial cultivation of human diploid cell strains. Exp. Cell Res. **25:**585–621.
20. **Herbert, B., A. E. Pitts, S. I. Baker, S. E. Hamilton, W. E. Wright, J. W. Shay, and D. R. Corey.** 1999. Inhibition of human telomerase in immortal human cells leads to progressive telomere shortening and cell death. Proc. Natl. Acad. Sci. USA **96:**14276–14281.
21. **Hockemeyer, D., A. J. Sfeir, J. W. Shay, W. E. Wright, and T. de Lange.** 2005. POT1 protects telomeres from a transient DNA damage response and determines how human chromosomes end. EMBO J. **24:**2667–2678.
22. **Johnson, R. T., and P. N. Rao.** 1970. Mammalian cell fusion: induction of premature chromosome condensation in interphase nuclei. Nature **226:**717–722.
23. **Kim, N. W., M. A. Piatyszek, K. R. Prowse, C. B. Harley, M. D. West, P. L. Ho, G. M. Coviello, W. E. Wright, S. L. Weinrich, and J. W. Shay.** 1994. Specific association of human telomerase activity with immortal cells and cancer. Science **266:**2011–2015.
24. **Lindsey, J., N. I. McGill, L. A. Lindsey, D. K. Green, and H. J. Cooke.** 1991. In vivo loss of telomeric repeats with age in humans. Mutat. Res. **256:**45–48.
25. **Maser, R. S., and R. A. DePinho.** 2004. Telomeres and the DNA damage response: why the fox is guarding the henhouse. DNA Repair (Amsterdam) **3:**979–988.
26. **Morin, G. B.** 1989. The human telomere terminal transferase enzyme is a ribonucleoprotein that synthesizes TTAGGG repeats. Cell **59:**521–529.
27. **O'Sullivan, J. N., M. P. Bronner, T. A. Brentnall, J. C. Finley, W. T. Shen, S. Emerson, M. J. Emond, K. A. Gollahon, A. H. Moskovitz, D. A. Crispin, J. D. Potter, and P. S. Rabinovitch.** 2002. Chromosomal instability in ulcerative colitis is related to telomere shortening. Nat. Genet. **32:**280–284.
28. **Ouellette, M. M., M. Liao, B. S. Herbert, M. Johnson, S. E. Holt, H. S. Liss, J. W. Shay, and W. E. Wright.** 2000. Subsenescent telomere lengths in fibroblasts immortalized by limiting amounts of telomerase. J. Biol. Chem. **275:**10072–10076.
29. **Pandita, T. K., S. Pathak, and C. R. Geard.** 1995. Chromosome end associations, telomeres and telomerase activity in ataxia telangiectasia cells. Cytogenet. Cell Genet. **71:**86–93.
30. **Pierce, A. J., R. D. Johnson, L. H. Thompson, and M. Jasin.** 1999. XRCC3 promotes homology-directed repair of DNA damage in mammalian cells. Genes Dev. **13:**2633–2638.
31. **Ramirez, R. D., B. S. Herbert, M. B. Vaughan, Y. Zou, K. Gandia, C. P. Morales, W. E. Wright, and J. W. Shay.** 2003. Bypass of telomere-dependent replicative senescence (M1) upon overexpression of Cdk4 in normal human epithelial cells. Oncogene **22:**433–444.
32. **Robles, S. J., and G. R. Adami.** 1998. Agents that cause DNA double strand breaks lead to p16INK4a enrichment and the premature senescence of normal fibroblasts. Oncogene **16:**1113–1123.
33. **Rogakou, E. P., D. R. Pilch, A. H. Orr, V. S. Ivanova, and W. M. Bonner.** 1998. DNA double-stranded breaks induce histone H2AX phosphorylation on serine 139. J. Biol. Chem. **273:**5858–5868.
34. **Rubelj, I., M. Huzak, B. Brdar, and O. M. Pereira-Smith.** 2002. A single-stage mechanism controls replicative senescence through sudden senescence syndrome. Biogerontology **3:**213–222.
35. **Rudolph, K. L., M. Millard, M. W. Bosenberg, and R. A. DePinho.** 2001. Telomere dysfunction and evolution of intestinal carcinoma in mice and humans. Nat. Genet. **28:**155–159.
36. **Serrano, M., A. W. Lin, M. E. McCurrach, D. Beach, and S. W. Lowe.** 1997. Oncogenic ras provokes premature cell senescence associated with accumulation of p53 and p16INK4a. Cell **88:**593–602.
37. **Sharma, G. G., A. Gupta, H. Wang, H. Scherthan, S. Dhar, V. Gandhi, G. Iliakis, J. W. Shay, C. S. Young, and T. K. Pandita.** 2003. hTERT associates with human telomeres and enhances genomic stability and DNA repair. Oncogene **22:**131–146.
38. **Sharma, G. G., K. K. Hwang, R. K. Pandita, A. Gupta, S. Dhar, J. Parenteau, M. Agarwal, H. J. Worman, R. J. Wellinger, and T. K. Pandita.** 2003. Human heterochromatin protein 1 isoforms HP1(Hsalpha) and HP1(Hsbeta) interfere with hTERT-telomere interactions and correlate with changes in cell growth and response to ionizing radiation. Mol. Cell. Biol. **23:**8363–8376.
39. **Shay, J. W., B. A. Van Der Haegen, Y. Ying, and W. E. Wright.** 1993. The frequency of immortalization of human fibroblasts and mammary epithelial cells transfected with SV40 large T-antigen. Exp. Cell Res. **209:**45–52.
40. **Shay, J. W., and W. E. Wright.** 1989. Quantitation of the frequency of immortalization of normal human diploid fibroblasts by SV40 large T-antigen. Exp. Cell Res. **184:**109–118.
41. **Smogorzewska, A., J. Karlseder, H. Holtgreve-Grez, A. Jauch, and T. de Lange.** 2002. DNA ligase IV-dependent NHEJ of deprotected mammalian telomeres in G1 and G2. Curr. Biol. **12:**1635–1644.
42. **Stansel, R. M., T. de Lange, and J. D. Griffith.** 2001. T-loop assembly in vitro involves binding of TRF2 near the 3′ telomeric overhang. EMBO J. **20:**5532–5540.
43. **Takai, H., A. Smogorzewska, and T. de Lange.** 2003. DNA damage foci at dysfunctional telomeres. Curr. Biol. **13:**1549–1556.
44. **van Steensel, B., A. Smogorzewska, and T. de Lange.** 1998. TRF2 protects human telomeres from end-to-end fusions. Cell **92:**401–413.
45. **Vaziri, H., and S. Benchimol.** 1998. Reconstitution of telomerase activity in normal human cells leads to elongation of telomeres and extended replicative life span. Curr. Biol. **8:**279–282.
46. **Veldman, T., K. T. Etheridge, and C. M. Counter.** 2004. Loss of hPot1 function leads to telomere instability and a cut-like phenotype. Curr. Biol. **14:**2264–2270.
47. **Wang, R. C., A. Smogorzewska, and T. de Lange.** 2004. Homologous recombination generates T-loop-sized deletions at human telomeres. Cell **119:**355–368.
48. **Weinrich, S. L., R. L. Pruzan, L. Ma, M. Ouellette, V. M. Tesmer, S. E. Holt, A. G. Bodnar, S. Lichtsteiner, N. W. Kim, J. B. Trager, R. B. Taylor, R. Carlos, W. H. Andrews, W. E. Wright, J. W. Shay, C. B. Harley, and G. B. Morin.** 1997. Reconstitution of human telomerase with the template RNA component hTR and the catalytic protein subunit hTRT. Nat. Genet. **17:**498–502.
49. **Wright, W. E., O. M. Pereira-Smith, and J. W. Shay.** 1989. Reversible cellular senescence: implications for immortalization of normal human diploid fibroblasts. Mol. Cell. Biol. **9:**3088–3092.
50. **Wright, W. E., and J. W. Shay.** 2002. Historical claims and current interpretations of replicative aging. Nat. Biotechnol. **20:**682–688.
51. **Wright, W. E., and J. W. Shay.** 2003. Telomeric shortening and replicative aging, p. 51–72. *In* F. M. Hisama, S. M. Weissman, and G. M. Martin (ed.), Chromosomal instability and aging: basic science and clinical implications. Marcel Dekker, Inc., New York, NY.
52. **Wright, W. E., and J. W. Shay.** 1995. Time, telomeres and tumors: is cellular senescence more than an anticancer mechanism? Trends Cell Biol. **5:**293–296.
53. **Wright, W. E., and J. W. Shay.** 1992. The two-stage mechanism controlling cellular senescence and immortalization. Exp. Gerontol. **27:**383–389.
54. **Zhang, X., V. Mar, W. Zhou, L. Harrington, and M. O. Robinson.** 1999. Telomere shortening and apoptosis in telomerase-inhibited human tumor cells. Genes Dev. **13:**2388–2399.
55. **Zhu, J., D. Woods, M. McMahon, and J. M. Bishop.** 1998. Senescence of human fibroblasts induced by oncogenic Raf. Genes Dev. **12:**2997–3007.
56. **Zou, Y., A. Sfeir, S. M. Gryaznov, J. W. Shay, and W. E. Wright.** 2004. Does a sentinel or a subset of short telomeres determine replicative senescence? Mol. Biol. Cell **15:**3709–3718.
57. **Zou, Y., X. Yi, W. E. Wright, and J. W. Shay.** 2002. Human telomerase can immortalize Indian muntjac cells. Exp. Cell Res. **281:**63–76.